Exciton mass increase in a GaAs/AlGaAs quantum well in a transverse magnetic field

S. Yu. Bodnar,[1] P. S. Grigoryev,[2] D. K. Loginov,[2] V. G. Davydov,[3] Yu. P. Efimov,[3] S. A. Eliseev,[3] V. A. Lovtcius,[3] E. V. Ubyivovk,[3,4] V. Yu. Mikhailovskii,[3] and I. V. Ignatiev[2]

[1]*Institut fur Physik, Johannes Gutenberg-Universitat, Staudinger Weg 7, 55128 Mainz, Germany*

[2]*Spin Optics laboratory, St-Petersburg State University, St-Petersburg, 198504, Russia*

[3]*St. Petersburg State University, 1, Ulianovskaya str., Petrodvorets, St. Petersburg, 198504, Russia*

[4]*ITMO University, 49 Kronverksky Pr., St. Petersburg, 197101, Russia*

(Received 9 November 2016; revised manuscript received 5 April 2017; published 22 May 2017)

In this work we have investigated the exciton reflectance spectra of a high quality heterostructure with a GaAs/AlGaAs quantum well in a transverse magnetic field (Voigt geometry). It has been shown that application of the magnetic field leads to a decrease of energy distance between spectral features related to the excitonlike polariton modes. This effect has been treated as the magneto-induced increase of the exciton mass. We have shown that the hydrogenlike and diamagnetic exciton models are insufficient to describe the exciton behavior in the intermediate magnetic fields studied. Considering the symmetry of the problem, we have developed a phenomenological model which adequately describes the experimental data.

DOI: 10.1103/PhysRevB.95.195311

I. INTRODUCTION

Effect of magnetic field on exciton states has been extensively studied for a long time, since the middle of the last century [1–7]. A pioneering work [1] demonstrated that the exciton lines reveal Zeeman splittings and diamagnetic shifts. In weak magnetic fields these effects can be described in the framework of a hydrogen model. However, a strong enough magnetic field significantly modifies exciton states giving rise to a so-called "diamagnetic exciton" [2–5] when the magnetic energy of moving carriers prevails over the Coulomb energy of their interaction. Subsequent studies have shown that the binding energy of diamagnetic excitons increases with the magnetic field rise [6,7].

Modern epitaxial technologies allow one to grow high-quality heterostructures for precise study of various effects. A number of magnetic-field-induced effects related to the quantum confinement of excitons has been predicted and found in different structures in the last two decades, see, e.g., Refs. [8–13]. In particular, in the paper by Lozovik *et al.* [8], the binding energy of indirect diamagnetic excitons in the double quantum wells (QWs) was studied as a function of the transverse magnetic field applied along the heterostructure layers. In Refs. [9,10] the effect of the magnetic field applied along or across the heterostructure growth axis was considered for both direct and indirect excitons in the double GaAs/AlGaAs QWs. The authors managed to experimentally observe and theoretically explain the behavior of spectral lines corresponding to the anticrossing of direct and indirect excitons induced by the variation of the magnetic field.

In the case of direct excitons, the QW-width dependence of the Zeeman splitting in the InGaAs/AlGaAs and GaAs/AlGaAs has been theoretically and experimentally studied in Refs. [11–15]. It was demonstrated that the variation of g-factors characterizing the splittings is caused by the heavy-hole-light-hole mixing. Similar study was done for excitons in the wurtzite GaN/AlGaN QWs as well as for charged excitons and for excitons localized at impurities in the asymmetrically doped GaAs/AlGaAs QWs [16–18]. In particular, a dependence of g factor on the magnetic field was observed and explained by the magnetic-field-induced mixing of heavy-hole and light-hole states.

Excitons in wide QWs in the external magnetic field is typically studied by reflectance spectroscopy [19–25]. This technique allows one to observe dozens of quantum confined exciton states in high-quality heterostructures and to restore the exciton dispersion introducing an effective wave vector for exciton propagation across the QW. It was found that the exciton propagation along the magnetic field (Faraday geometry) leads to the Zeeman splitting of exciton states, in which magnitude depends on the wave vector [20–23]. The application of the magnetic field perpendicular to the direction of the exciton propagation (Voigt geometry) results in a modification of the exciton dispersion, which is discussed in several works [19,24–26]. Magnetic-field-induced effects have been studied for several different types of heterostructures but, in the case of the GaAs/AlGaAs QWs, these effects have been studied only in the Faraday geometry [15,20].

This work is devoted to the study of the exciton dispersion in a wide GaAs/AlGaAs QW in the transverse magnetic field (Voigt geometry). Similar to works [19,20,22,24,25], the exciton dispersion is obtained from reflectance spectra of the structure. Theoretical analysis of the magnetic-field-induced modification of the exciton dispersion encounters certain difficulties. Particularly, it has been found that theoretical models used in Refs. [19,20,22,24–26] are not suitable for analysis of the exciton dispersion in the moderate magnetic fields 0–3 T used in our experiments. In the cited works, the approximation of a weak magnetic field has been exploited. The hydrogenlike exciton wave functions were considered as the basic set for the problem and the magnetic field effects were analyzed in the framework of perturbation theory. However, in our case, the magnetic field cannot be considered as a weak one.

The exciton state in the opposite extreme of the strong magnetic field can be described in the framework of the diamagnetic exciton model [2–5,27–29]. It assumes that the magnetic-field-induced changes of exciton energy is considerably stronger than the Coulomb energy of the electron-hole

interaction. The unperturbed exciton Hamiltonian includes operators, which depend on the magnetic field, and the Coulomb interaction is considered as a perturbation. As it will be shown below, this model is also not accurate enough to describe the magnetic-field-induced effects we discuss in the present work. Namely, the exciton energy corrections induced by the magnetic field are comparable with the Coulomb energy of the electron-hole interaction so that the approximation of a diamagnetic exciton does not fit the experimental conditions. In other words, the nonadiabatic corrections in such an *intermediate* magnetic field cannot be considered as small ones [2]. An analytical solution of the problem taking into account the nonadiabatic corrections has not been found yet.

For the analysis of our experimental data, we use the diamagnetic exciton model as a zero approximation. In order to include the nonadiabatic corrections to this approximation, we consider quantum characteristics of the diamagnetic exciton states as fitting parameters. These parameters are determined by comparison with the experimental data. They can be used to estimate the deviation from the diamagnetic exciton model. In order to model the dependence of these fitting parameters on external magnetic field **B** and on exciton wave vector **K**, we exploit the invariant method (see, e.g., textbooks [30,31]).

The rest of the paper is organized as follows. In Sec. II we describe the experimental results on reflectance spectra and their phenomenological analysis. In Sec. III we discuss the approximations of strong and weak magnetic fields as well as their limitations in the description of exciton behavior in our experiments. Also in this section we propose a generalized diamagnetic exciton model for the case of intermediate magnetic fields in the framework of the invariance method. The main conclusions are given in Sec. IV.

II. POLARITON REFLECTANCE SPECTRA

In the present work we study the magnetic-field-induced modification of the exciton dispersion by reflectance spectroscopy for a heterostructure with a wide GaAs/AlGaAs QW. The heterostructure was grown by molecular beam epitaxy on the [001] GaAs substrate. It contains the wide QW and several technological layers of AlGaAs and AlAs, grown to prevent the dislocation growth throughout the structure. Optical response from the wide QW under study is not hindered in any way by other layers of the structure, as they do not have resonance states in the energy range of interest. Due to the gradient of layer thicknesses, the actual thickness of the QW layer was determined by transmission electron microscopy (TEM). To minimize the error in the determination of layer thickness, the TEM measurements were done near the point at the sample surface where the reflectance spectra have been measured. The measured thickness of the QW layer, $L_{QW} = 225$ nm, is found to be slightly smaller than the nominal thickness 240 nm set in the growth program for the structure.

The reflectance spectra are measured at the nearly normal incidence of the light beam to the sample surface (z axis). The magnetic field was directed along the $[1\bar{1}0]$ crystal axis (x axis) that is perpendicular to the light beam (Voigt geometry). The sample was placed in a continuous-flow cryostat and held at temperature $T = 1.5$ K. We used a femtosecond titanium-sapphire laser as a light source with

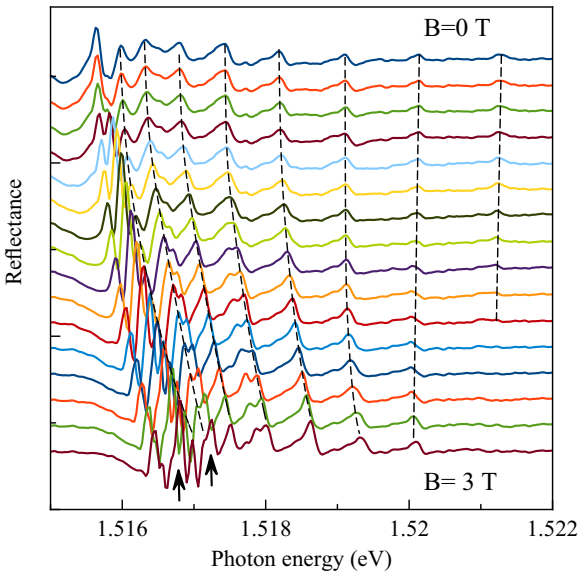

FIG. 1. Reflectance spectra of the heterostructure with QW, $L_{QW} = 225$ nm, measured in the transverse magnetic field, varied from $B = 0$ up to $B = 3$ T with step $\Delta B = 0.2$ T. The magnetic field is applied along the $[1\bar{1}0]$ crystal axis. Incident light is polarized across the magnetic field direction. Dashed lines show the magnetic-field-induced shift of polaritonic resonances. Arrows point out the spectral peculiarities appearing in the magnetic field.

emission spectrum covering the spectral range of the investigated polariton resonances. To avoid the resonance broadening due to exciton-exciton scattering, we used a low excitation power ($\sim 10^{-3}$ W/cm^2) [32].

The reflectance spectra are measured for two linear polarizations of incident light, namely, along and transverse to the direction of the magnetic field. Since we found no principal difference between the spectra, we consider only the reflectance spectra measured in polarization perpendicular to the magnetic field.

Reflectance spectra for a variety of magnetic field values are shown in Fig. 1. We attribute the peculiarities observed in the spectra mainly to the heavy-hole exciton polaritons inside the QW. The contribution of the light-hole excitons is considerably smaller [33]. The strongest peculiarities correspond to the anticrossing of the exciton and photon modes. The quasiperiodic oscillations lying higher in energy can be attributed to the standing polariton waves with wave vectors much larger that the light wave vector (see details in Refs. [20,34–36]). These oscillations can be treated as a polarization inside the QW, governed by the quantum-confined exciton states [37].

Figure 1 clearly demonstrates the two main effects of the magnetic field. First, there is a systematic energy shift of spectral features related to the diamagnetic shift of exciton states. The second effect is the decrease of the energy difference between spectral features with increasing magnetic field. These changes are related to the modification of the exciton dispersion in the magnetic field discussed below.

Beside these two main effects, there are also several other effects induced by the magnetic field. A strong modification of the spectra is observed in the lower energy range. In particular, new peculiarities appear with the magnetic field rise. Two of

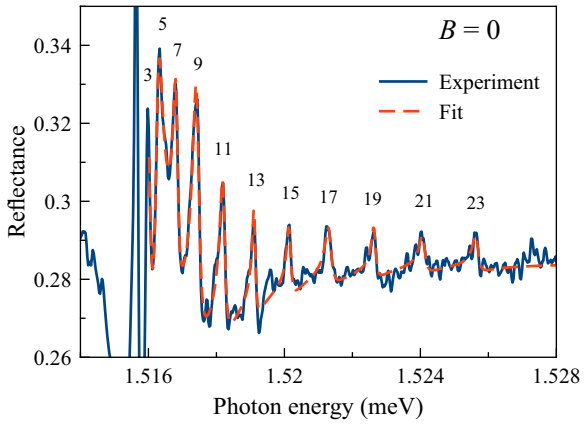

FIG. 2. Reflectance spectrum measured at zero magnetic field (noisy curve) and its fit by Eqs. (1) and (2) (dashed curve). Numbers indicate the quantum-confined exciton states.

them are indicated by arrows in Fig. 1. These peculiarities may be attributed to the light-hole excitons, whose exciton-light coupling increases due to their mixing with the radiative heavy-hole excitons [16]. Another effect is a variation of amplitudes of exciton resonances. For example, the intensities of low-energy resonances increase with the magnetic field, while the resonances with energy $E > 1.52$ eV almost disappear at a relatively strong magnetic field. We do not discuss these effects in the present paper in detail.

For a quantitative analysis of the two main effects described above, the actual energy position of the quantum-confined exciton states should be carefully determined from the experimental spectra. Consider exciton resonances in the spectrum at zero magnetic field, shown in Fig. 2. Each resonance is an asymmetric contour, so the actual position of the state may deviate from the position of the resonant peak. The high-energy resonances are relatively weak and noisy, therefore an accurate determination of their position also requires approximation with an analytical function.

We used a model described in the textbook by Ivchenko [28] and generalized in Ref. [38] for simulation of several well spectrally separated exciton resonances. General expressions for the reflectance spectrum are [38]

$$R(\omega) = \left| \frac{r_{01} + r_{\mathrm{QW}} e^{2i\phi}}{1 + r_{01} r_{\mathrm{QW}} e^{2i\phi}} \right|, \tag{1}$$

$$r_{\mathrm{QW}} = \sum_{N=1}^{N_{\max}} \frac{i(-1)^{(N-1)} \Gamma_{0N} e^{i\varphi_N}}{(\omega_{0N} - \omega) - i(\Gamma_{0N} + \Gamma_N)}. \tag{2}$$

Here ω_{0N} is the frequency of the Nth exciton transition, Γ_{0N} is the exciton decay rate, and Γ_N is the rate of various scattering processes broadening the exciton resonance. Phases φ_N are governed by the QW potential and may differ for different resonances in case of the asymmetric QW potential [39]. Phase ϕ describes the phase of electromagnetic wave acquired during propagation from the sample surface to the QW. Parameter r_{01} describes the amplitude reflection from the sample surface.

In wide QWs, low-energy quantum-confined exciton states are close to each other and the interaction with light may couple these states. In this case the model described by Eqs. (1) and (2) is not applicable and a more general model should be used [40]. To simplify the problem, we use Eqs. (1) and (2) for excited exciton states only, for which the coupling is negligibly small. An example of the reflectance spectrum simulation is shown in Fig. 2. In the simulation we fixed phases φ_N almost for all resonances, $\varphi_N = 3.8$, because the asymmetry of QW potential is negligibly small for wide QWs. The exception is the phase for the lowest resonance involved into the fit $\varphi_5 = 2.2$. It is affected by low-energy resonances.

As seen in Fig. 2, the simulation accurately reproduces exciton resonances in a wide spectral range [41]. This simulation allows us to precisely determine the exciton energies. We found that there is a small systematic energy shift $\delta E_N \approx 30$ μeV of the exciton energy position determined by the simulation from the position of resonant maximum. The spread of this shift is smaller than 10 μeV. We, therefore, may use a "naive" method of determination of the exciton energy as the position of resonant maximum with the systematic shift added. We used this method if the additional resonances appearing in the magnetic field hindered the accurate simulation of reflectance spectra.

The exciton resonances in wide QWs typically correspond to optical transitions to even or odd quantum-confined exciton states [36,37]. The oscillator strength for other transitions (odd or even, respectively) is much smaller. They can be seen as small peculiarities between the main resonances in Fig. 2.

The identification of resonances is based on two assumptions well verified for wide QWs [35,37]. First, the exciton dispersion is weakly affected by the QW interfaces and, therefore, one can use the dispersion for bulk crystal. Far beyond the anticrossing point, it is described by a parabolic dependence on the exciton wave vector K:

$$E = \frac{\hbar^2 K^2}{2M} + E_X. \tag{3}$$

Here E_X is the exciton ground state energy and M is the exciton mass $M = m_e + m_h$, where m_e and m_h are the effective masses of electron and hole, respectively. Second, the observed exciton resonances correspond to the quantization of the center-of-mass exciton motion described by the discrete values of exciton wave vector:

$$K_N = \pi N / L^*_{\mathrm{QW}}, \tag{4}$$

where N is the number of the quantum confined exciton state. The effective thickness of QW, L^*_{QW}, differs from the real QW thickness L_{QW} by the double value of a transition layer [42] frequently called a "dead layer" L_D [43–46]. The latter parameter depends on the QW thickness and, for $L_{\mathrm{QW}} =$ 225 nm, its value $L_D \approx 15$ nm [45,46]. Correspondingly, the effective thickness of the QW under study, $L^*_{\mathrm{QW}} = L_{\mathrm{QW}} - 2L_D = 195$ nm, with accuracy of a few nm.

The analysis shows that the energy positions of exciton resonances are well described by Eqs. (3) and (4). The exciton dispersion restored using these equations is shown in Fig. 3. We used effective masses $m_e = 0.067\ m_0$ and $m_h = 0.45\ m_0$, where m_0 is the free electron mass. This modeling also allows one to assign certain numbers of the quantum-confined exciton states to the exciton resonances observed (see Fig. 2). We should note that number N cannot be directly found from the

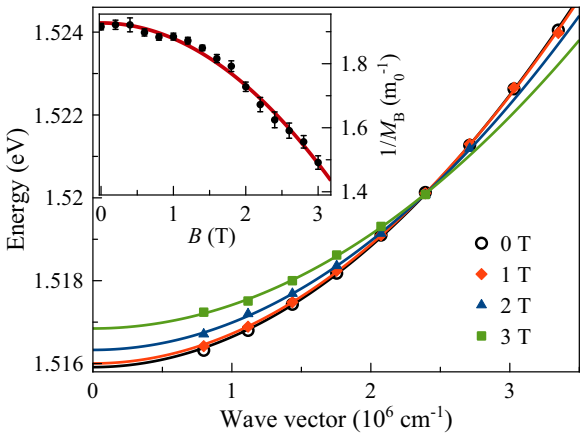

FIG. 3. Exciton dispersion curves for several values of the magnetic field. Symbols are the experimental data and the curves are fits by formula (3). Inset shows the dependence of inverse exciton mass $1/M(B)$ on the magnetic field. Points are the values extracted from the fit of dispersion data and the solid curve is the approximation by formula (5).

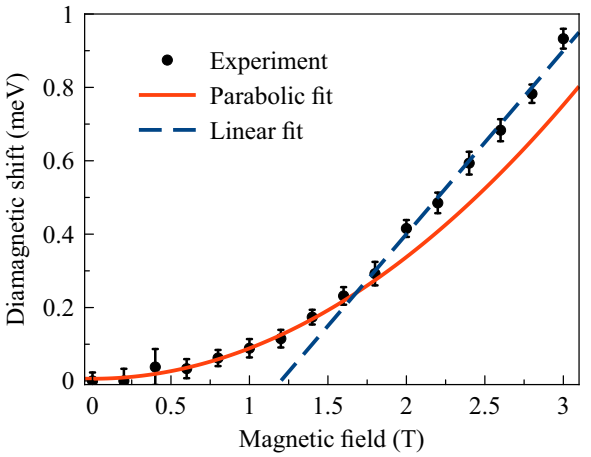

FIG. 4. Dependence of the diamagnetic shift ΔE_X on the magnetic field. Points show values of ΔE_X obtained from the fit of dispersion curves by Eq. (3). Red solid curve is the fit by parabolic dependence (6) with $D_2 = 0.085$ meV/T^2 in the range $0 < B < 1.5$ T. Blue dashed line is the fit by linear dependence (7) with $D_1 = 0.49$ meV/T and $D_0 = -0.57$ meV for $B > 1.5$ T.

experimental spectra because of dense exciton peculiarities near the exciton-photon anticrossing point (see Fig. 1).

Similar analysis of reflectance spectra was performed for the case of nonzero magnetic field. As it is shown in the next section, the exciton dispersion should remain parabolic with increasing magnetic field. It can be described by Eqs. (3) and (4) if the exciton mass and the exciton energy are considered depending on the magnetic field $M(B)$ and $E_X(B)$. In the phenomenological analysis of reflectance spectra, we assign simple fit functions to these quantities. Using the appropriate fitting parameters one can describe spectral positions of exciton resonances using Eqs. (3) and (4) and, hence, determine the exciton dispersion for each particular value of the magnetic field.

Examples of the dispersion curves are shown in Fig. 3. The curvature of dispersion curves clearly decreases with the magnetic field, which indicates the increase of exciton mass $M(B)$. Respective values of the inverse exciton mass $1/M(B)$ as a function of B obtained by fitting the dispersion curves with Eq. (3) are given in the inset of the figure. The dependence is well fitted by a parabolic function:

$$\frac{1}{M(B)} = \frac{1}{M} - D_M B^2. \tag{5}$$

Fitting parameter $D_M = (0.048 \pm 0.002)\, m_0^{-1}\,\mathrm{T}^{-2}$, where m_0 is the free electron mass.

Beside the exciton mass variation, a diamagnetic shift of the exciton ground state,

$$\Delta E_X(B) = E_X(B) - E_X(0),$$

was determined from the dispersion curves. We should note that the accuracy of the shift determination is limited because it is found using a limited number of experimental points. The direct determination of this shift from the experimental spectra, however, is even more problematic because of the complex structure of the spectral features at the anticrossing point, which is, in addition, strongly modified by the magnetic field, see Fig. 1.

The diamagnetic shift $\Delta E_X(B)$ obtained by the extrapolation procedure is shown in Fig. 4. According to the models of the hydrogenlike [26,47] and diamagnetic excitons [2,4], the diamagnetic shift should quadratically depend on the magnetic field at $B \ll B_L$ and should tend to a linear dependence at large B. Here B_L is a critical magnetic field, at which the cyclotron energy of electron-hole pair becomes equal to their Coulomb energy in the hydrogenlike exciton (see next section for details). For the case of an exciton in GaAs, $B_L \approx 4$ T. We, therefore, fit the diamagnetic shift for $B < 1.5$ T by a parabolic dependence:

$$\Delta E_X(B) = D_2 B^2, \tag{6}$$

with fitting parameter $D_2 = (0.085 \pm 0.004)$ meV/T^2. For $B > 1.5$ T, we use a linear dependence of ΔE_X:

$$\Delta E_X(B) = D_1 B + D_0. \tag{7}$$

The fitting parameters are $D_1 = (0.49 \pm 0.02)$ meV/T and $D_0 = (-0.57 \pm 0.04)$ meV. As seen in Fig. 4, functions (6) and (7) well fit the experimental dependence in the respective magnetic field ranges. At the same time, the obtained values of fitting parameters D_2 and D_1 do not agree with those calculated in the framework of the hydrogenlike and diamagnetic models, which is discussed in the next section.

III. EXCITON IN MAGNETIC FIELD

For quantitative analysis of exciton energy, we choose a coordinate system in which the x axis is directed along the magnetic field so that $B = B_x$. We also choose this direction as the quantization axis for the angular momenta. We consider the excitons propagating along the z axis that is $K = K_z$. This direction coincides with the growth axis of the heterostructure. The total Hamiltonian of an exciton in the magnetic field consists of the Hamiltonians for a free hole (the Luttinger

Hamiltonian) and for a free electron, as well as of an operator of their Coulomb interaction.

The analytical solution of Schrödinger equation with this Hamiltonian is not possible in the general case. Two approximations, the hydrogenlike model and the model of diamagnetic exciton mentioned above, are typically used for weak and strong magnetic fields, respectively. The criterion of a strong magnetic field has been proposed by Elliott and Loudon [2] and generalized by Zhilich and Monozon [48] for excited exciton states:

$$\beta_n = \frac{\hbar\Omega}{2R_X}n^2 = \frac{\varepsilon_0^2\hbar^3 B}{\mu^2 e^3 c}n^2 \gg 1. \tag{8}$$

Here $\Omega = |e|B/(\mu c)$ is the sum of cyclotron frequencies of a free electron and a hole, n is the principal quantum number of an exciton state in the hydrogenlike model, and $R_X = \mu e^4/(2\hbar^2\varepsilon_0^2)$ is the binding energy for an exciton state with $n = 1$ (exciton Rydberg). In formula (8), $\mu = m_h m_e/(m_h + m_e)$ is the reduced exciton mass, where $m_e = 0.067\ m_0$ and $m_h = m_0/(\gamma_1 - 2\gamma_2) = 0.45\ m_0$ are the effective masses of an electron and a hole in GaAs, respectively [49]; m_0 is the free electron mass, γ_1, γ_2 are the Luttinger parameters, e is the electron charge, $\varepsilon_0 = 12.56$ is the permittivity of GaAs crystal [50], and c is the speed of light. In particular, for the ground exciton state ($n = 1$) in GaAs, $\beta = 1$ for the magnetic field $B_L \approx 4$ T.

A. Weak magnetic field

First, we consider an approximation of the weak magnetic field $\beta_n \ll 1$ when the Coulomb interaction of a hole and an electron in the exciton is much stronger than the interaction with the magnetic field. The hydrogenlike Hamiltonian in zero magnetic field can be used as the nonperturbed Hamiltonian in this case. The nonperturbed exciton states are described by the principal quantum number n. The effect of the magnetic field on the exciton energy is usually calculated in the framework of the first and higher orders of perturbation theory [19,24–26]. Particularly, the magnetic field mixes the ground $1s$ state with an infinite number of the hydrogenlike p states of the discrete energy spectrum as well as with the states of a continuum [26].

The binding energy of hydrogenlike exciton states rapidly decreases with n as $1/n^2$. Therefore, even for a small, but nonzero, magnetic field, the criterion of a strong magnetic field (8) can be fulfilled for large enough n. For example, the criterion (8) is fulfilled for states with $n \geqslant 2$ in the magnetic field $B > 1$ T. Thus, the description of the magnetic field effects in the framework of the hydrogenlike exciton model and of the perturbation theory becomes inapplicable for relatively low magnetic fields.

Let us consider, e.g., the diamagnetic shift of the lowest $1s$-exciton state shown in Fig. 4. In the framework of hydrogenlike model, it is described by a parabolic dependence, similar to Eq. (6), with coefficient $D_2^{(\mathrm{H})}$ determined by expression [26,47]

$$D_2^{(\mathrm{H})} = \frac{1}{4}\left(\frac{m_e^2}{m_h} + \frac{m_h^2}{m_e}\right)\left(\frac{ea_B}{Mc}\right)^2. \tag{9}$$

Here $a_B = \hbar^2\varepsilon_0/(\mu e^2)$ is the exciton Bohr radius. For GaAs this expression gives $D_2^{(\mathrm{H})} = 0.065$ meV/T^2. This value is considerably smaller than that obtained from the fit of experimental data shown in Fig. 4, $D_2 = 0.085$ meV/T^2. This discrepancy points out that even the range $0 < B < 1.5$ T used in the fit cannot be considered as the range of small enough magnetic fields for excitons in GaAs.

The approximation of a strong field is also not totally applicable. Indeed, according to Refs. [3,28], the energy of lowest state of the diamagnetic exciton should linearly depend on the magnetic field with factor $D_1^{(\mathrm{DM})} = \hbar\Omega/(2B) = e\hbar/(2\mu c) \approx 1$ meV/T for GaAs. The fit of experimental data gives smaller factor $D_1 = 0.49$ meV/T (see Fig. 4).

These estimates show that both limits, the weak and the strong magnetic fields, cannot be applied to describe the experimentally observed behavior of the diamagnetic shift and we should speak about an intermediate magnetic field. Because there is no simple theoretical model for this case [51], we consider a phenomenological approach based on the model of a diamagnetic exciton as a zero approximation. Then we consider some parameters of the model as the fitting parameters to take into account that the adiabatic approximation (see, e.g., Refs. [2,5]) is broken for the intermediate magnetic fields.

B. Intermediate magnetic field

In the framework of the diamagnetic exciton model, relative motions of electrons and holes along and across the magnetic field are considered to be adiabatically independent, because the motion across the magnetic field is much faster than along it, see, e.g., Refs. [3,28]. The motion across the magnetic field is governed by the interaction of an electron and a hole with the magnetic field because their Coulomb interaction is negligibly small. The Hamiltonian describing this motion is

$$\hat{H}_\perp = -\frac{\hbar^2}{2\mu}\left\{\frac{1}{\rho}\frac{\partial}{\partial\rho}\left(\rho\frac{\partial}{\partial\rho}\right) + \frac{1}{\rho^2}\frac{\partial^2}{\partial\varphi^2}\right\} - \frac{eB\hbar}{2\mu c}\frac{\partial}{\partial\varphi} + \frac{e^2B^2\rho^2}{8\mu c^2}, \tag{10}$$

where $\rho^2 = y^2 + z^2$ is the distance between an electron and a hole in the yz plane, which is perpendicular to the magnetic field.

A general expression for respective wave functions has the form [6,28,29]

$$\mathrm{R}_N^m = \frac{1}{\lambda_B}\frac{e^{im\varphi}}{\sqrt{2\pi}}\sqrt{\frac{N!}{(N+|m|)!}}e^{-\eta/2}\eta^{|m|/2}L_N^{|m|}(\eta). \tag{11}$$

Here $\lambda_B = \sqrt{(\hbar c)/(eB)}$ is the magnetic length, $\eta = \rho^2/(2\lambda_B^2)$, and functions $L_N^{|m|}(\eta)$ are the associated Laguerre polynomials. Quantities N and $m = -N, \ldots, N$ are the quantum numbers of Landau bands and subbands, respectively. The energy of the relative electron-hole motion perpendicular to the external magnetic field is

$$E_c = \hbar\Omega\left(N + \frac{|m| + \gamma m + 1}{2}\right), \tag{12}$$

where γ is of order of unity [29]. This expression describes the diamagnetic shift of state with numbers (N, m). We should note that the excited states of a diamagnetic exciton with

$N > 0$ give a small contribution into the reflectance spectra in comparison with the lowest state ($N = 0$, $m = 0$) and we may not consider them. At the same time, the diamagnetic shift of the lowest state calculated with $N = 0$ does not agree with the experiment in our case of the intermediate magnetic fields as it is already discussed above in this section. This deviation is caused by an effect of the Coulomb interaction on the relative electron-hole motion in the plane perpendicular to the magnetic field. We should stress that, in the case of a strong magnetic field ($\beta \gg 1$), the Coulomb-interaction related corrections of exciton energy become negligibly small [2].

To describe the experimentally observed diamagnetic shift, we save N in Eq. (12) and consider it as a fitting parameter. Its value can be found comparing this expression with a linear approximation (7) of the diamagnetic shift $N = (D_1/D_1^{(\mathrm{DM})} - 1)/2 = -0.25$. The deviation of this parameter from zero, which should be for the purely diamagnetic exciton, is not large as compared to unity. In other words, the Coulomb interaction causes relatively weak coupling of the diamagnetic exciton states with $N = 0$ and $N = 1$ at magnetic fields $B > 1.5$ T. This fact justifies the suggested phenomenological approach.

The relative electron-hole motion along the magnetic field is described by Hamiltonian

$$\hat{H}_{||} = -\frac{\hbar^2}{2\mu}\frac{\partial^2}{\partial x^2} + V_{N,m}(x). \tag{13}$$

Here $V_{N,m}(x) = \langle \mathrm{R}_N^m | e^2/(\varepsilon_0 r) | \mathrm{R}_N^m \rangle$ is the one-dimensional Coulomb potential for the relative electron-hole motion, $r = \sqrt{\rho^2 + x^2}$, and x is the electron-hole distance in the x direction that is along the magnetic field.

The exact analytical expression for this potential is too complex and its substitution into the Schrödinger equation does not allow one to obtain any analytical solution of the problem. However, for $N = 0$ and $m = 0$, this potential is well approximated by a simple function [3]:

$$V_{1d} = -\frac{e^2}{\varepsilon_0(a + |x|)} + \frac{A^2 e^2 a}{\varepsilon_0(a + |x|)^2}. \tag{14}$$

Here a and A are the fitting parameters. The relative motion in such a potential is described by the Whittaker function $W_{\alpha,\nu}$, where index α is the state number for the one-dimensional exciton determined from the matching conditions at point $x = 0$; index $\nu = \sqrt{1/4 + 2Aa/a_B}$ [3].

The energy of relative electron-hole motion along the magnetic field in such a potential, that is the exciton binding energy, can be expressed as [3]

$$\mathcal{R}_X = \frac{R_X}{\alpha^2}. \tag{15}$$

This energy slowly (sublinearly) depends on the magnetic field [7,28,52]. Besides, it should also depend on the exciton wave vector K. This dependence has not been analyzed in detail so far. In the case of intermediate magnetic fields and relatively small wave vectors ($K \ll \pi/a_0$, where a_0 is a lattice constant), $\mathcal{R}_X$ can be expanded in a series in powers of K and B, which satisfy the symmetry of the system in the Γ point of Brillouin zone for GaAs [30,31]. The symmetry permits any even powers of B and K, including zero and negative powers, therefore we should consider some physical arguments to choose the terms in the series required for the following analysis.

The exciton motion across the magnetic field gives rise to an appearance of an effective electric field $\mathbf{F}_{\mathrm{eff}} = \hbar[\mathbf{K} \times \mathbf{B}]/(Mc)$, acting on the electron and the hole in the reference frame of the exciton center-of-mass [6]. This electric field increases the exciton binding energy due to the quadratic Stark effect [53,54] when it is relatively small, $eF_{\mathrm{eff}}a_B/R_X \ll 1$. It is important that $F_{\mathrm{eff}} \propto KB$, therefore we expand $\mathcal{R}_X$ in series in $(KB)^{2n}$ and consider only first two terms:

$$\mathcal{R}_X = R_X(1 + \xi_2 K^2 B^2). \tag{16}$$

Here R_X is the exciton binding energy at zero wave vector and ξ_2 is a fitting parameter.

The total wave function of a diamagnetic exciton can be presented as

$$\Psi = \mathrm{R}_N^m(\rho) W_{\alpha,\nu}(x) e^{iKz}, \tag{17}$$

where function e^{iKz} describes the motion of the exciton as a whole particle. The total exciton energy is described as a sum of the internal energy of the exciton, expressions (12) and (16), and of the exciton kinetic energy:

$$E = \hbar\Omega\left(N + \frac{1}{2}\right) - R_X(1 + \xi_2 K^2 B^2) + \frac{\hbar^2 K^2}{2M}. \tag{18}$$

Combining the last term in this expression describing the kinetic energy with the second term in Eq. (16), we obtain

$$E = \hbar\Omega\left(N + \frac{1}{2}\right) - R_X + \frac{\hbar^2 K^2}{2M}(1 - \xi_M B^2), \tag{19}$$

where $\xi_M = \xi_2 R_X (2M/\hbar^2)$. The last term in this expression can be treated as the kinetic energy of an exciton with an effective mass depending on the magnetic field:

$$\frac{1}{M(B)} = \frac{1}{M}\left(1 - \frac{2\xi_2 R_X}{\hbar^2} M B^2\right) = \frac{1}{M}(1 - \xi_M B^2). \tag{20}$$

Comparing this expression with Eq. (5), we can determine the value of parameter $\xi_M = D_M M = 0.025\ \mathrm{T}^{-2}$. We should note that, at the maximal magnitude of magnetic field used in the experiments, $B = 3$ T, the second term in expression (20), $\xi_M B^2 = 0.23$, that is considerably smaller than unity. This confirms the applicability of expansion (16) in the case of intermediate magnetic fields considered here.

The change of exciton mass in the intermediate magnetic fields can be treated as the magnetic-field-induced coupling of the relative electron-hole motion with the exciton motion as a particle. We should note that, in the weak magnetic fields when the hydrogenlike exciton model is applicable, the modification of exciton mass is also caused by the magnetic-field-induced coupling of the relative electron-hole motion and the exciton motion as a whole [24,26]. This coupling also results in a parabolic dependence of the inverse exciton mass on the magnetic field. We therefore may expect a parabolic dependence in the whole range of magnetic fields studied. Good approximation of the experimental data shown in the inset of Fig. 3 by the parabolic dependence (5) confirms this conclusion.

IV. CONCLUSION

We experimentally studied and theoretically analyzed polariton reflectance spectra of a heterostructure with a wide GaAs/AlGaAs QW in the transverse magnetic field varied from zero to 3 T. We observed the magnetic-field-induced modification of the exciton dispersion, which is detected as a decrease of energy distance between exciton resonances related to the quantum-confined exciton states in the QW. The modification of the dispersion is treated as an increase of mass of the heavy-hole exciton. The theoretical analysis is based on the model of a diamagnetic exciton. In order to apply the model to the case of intermediate magnetic fields, we used some parameters of the model as the fitting parameters. This approach allowed us to describe the experimentally observed quadratic in the magnetic field decrease of inverse exciton mass and the linear diamagnetic shift of the exciton ground state in magnetic fields $1.5 < B < 3$ T. The development of a microscopic model, which could describe these effects, needs further theoretical study.

ACKNOWLEDGMENTS

This work was supported by the Russian Foundation for Basic Research (Grant No. 16-02-00245 a). The studied heterostructure was grown in the resource Centre "Nanophotonics" and the microscopic data were obtained using the equipment of the Interdisciplinary Resource Centre for Nanotechnology of St. Petersburg State University.

[1] E. F. Gross and B. P. Zakharchenya, Linear and quadratic Zeeman effect and diamagnetism of exciton in cuprous oxide crystal, Dokl. Akad. Nauk SSSR **111**, 564 (1956).

[2] R. J. Elliott and R. Loudon, Theory of fine structure on the absorption edge in semiconductors, J. Phys. Chem. Solids **8**, 382 (1959).

[3] R. J. Elliott and R. Loudon, Theory of the absorption edge in semiconductors in a high magnetic field, J. Phys. Chem. Solids **15**, 196 (1960).

[4] R. P. Seisyan, Diamagnetic excitons and exciton magnetopolaritons in semiconductors, Semicond. Sci. Technol. **27**, 053001 (2012).

[5] R. P. Seisyan, Diamagnetic excitons in semiconductors (Review), Fiz. Tverd. Tela **58**, 833 (2016) [Phys. Solid State **58**, 859 (2016)].

[6] L. P. Gor'kov and I. E. Dzyaloshinskii, Contribution to the theory of the Mott exciton in a strong magnetic field, Zh. Eksp. Teor. Fiz. **53**, 717 (1967) [Sov. Phys. JETP **26**, 449 (1968)].

[7] I. V. Lerner and Yu. E. Lozovik, Mott exciton in quasi two-dimensional semiconductors in high magnetic fields, Zh. Eksp. Teor. Fiz. **78**, 1167 (1978) [Sov. Phys. JETP **51**, 588 (1980)].

[8] Yu. E. Lozovik, I. V. Ovchinnikov, S. Yu. Volkov, L. V. Butov, and D. S. Chemla, Quasi-two-dimensional excitons in finite magnetic fields, Phys. Rev. B **65**, 235304 (2002).

[9] M. de Dios-Leyva, C. A. Duque, and L. E. Oliveira, Calculation of direct and indirect excitons in GaAs/Ga_{1-x} Al_xAs coupled double quantum wells: The effects of in-plane magnetic fields and growth-direction electric fields, Phys. Rev. B **76**, 075303 (2007).

[10] A. L. Morales, N. Raigoza, C. A. Duque, and L. E. Oliveira, Effects of growth-direction electric and magnetic fields on excitons in GaAs-$Ga_{1-x}Al_x$As coupled double quantum wells, Phys. Rev. B **77**, 113309 (2008).

[11] R. Kotlyar, T. L. Reinecke, M. Bayer, and A. Forchel, Zeeman spin splittings in semiconductor nanostructures, Phys. Rev. B **63**, 085310 (2001).

[12] Y. H. Chen, X. L. Ye, B. Xu, Z. G. Wang, and Z. Yang, Large g factors of higher-lying excitons detected with reflectance difference spectroscopy in GaAs-based quantum wells, Appl. Phys. Lett. **89**, 051903 (2006).

[13] A. Arora, A. Mandal, S. Chakrabarti, and S. Ghosh, Magneto-optical Kerr effect spectroscopy based study of Lande g-factor for holes in GaAs/AlGaAs single quantum wells under low magnetic fields, J. Appl. Phys. **113**, 213505 (2013).

[14] V. V. Solovyev, V. A. Bunakov, S. Schmult, and I. V. Kukushkin, Light-hole quantization in the optical response of ultra-wide GaAs/Al_xGa_{1-x}As quantum wells, J. Phys.: Condens. Matter **25**, 025801 (2013)

[15] P. S. Grigoryev, O. A. Yugov, S. A. Eliseev, Yu. P. Efimov, V. A. Lovtcius, V. V. Petrov, V. F. Sapega, and I. V. Ignatiev, Inversion of Zeeman splitting of exciton states in InGaAs quantum wells, Phys. Rev. B **93**, 205425 (2016).

[16] W. Bardyszewski and S. P. Lepkowski, Nonlinear Zeeman splitting of magnetoexcitons in c-plane wurtzite GaN-based quantum wells, Phys. Rev. B **90**, 075302 (2014).

[17] J. Jadczak, M. Kubisa, K. Ryczko, L. Bryja, and M. Potemski, High magnetic field spin splitting of excitons in asymmetric GaAs quantum wells, Phys. Rev. B **86**, 245401 (2012).

[18] J. Jadczak, L. Bryja, K. Ryczko, M. Kubisa, A. Wjs, M. Potemski, F. Liu, D. R. Yakovlev, M. Bayer, C. A. Nicoll, I. Farrer, and D. A. Ritchie, High magnetic field studies of charged exciton localization in GaAs/$Ga_{1-x}Al_x$As quantum wells, Appl. Phys. Lett. **105**, 112104 (2014).

[19] D. Loginov, V. P. Kochereshko, A. Litvinov, L. Besombes, H. Mariette, J. J. Davies, L. C. Smith, and D. Wolverson, Excitonic polaritons in transverse magnetic fields, Acta Phys. Pol. A **112**, 381 (2007).

[20] J. J. Davies, D. Wolverson, V. P. Kochereshko, A. V. Platonov, R. T. Cox, J. Cibert, H. Mariette, C. Bodin, C. Gourgon, E. V. Ubylvovk, Y. P. Efimov, and S. A. Eliseev, Motional Enhancement of Exciton Magnetic Moments in Zinc-Blend Semiconductors, Phys. Rev. Lett. **97**, 187403 (2006).

[21] L. C. Smith, J. J. Davies, D. Wolverson, S. Crampin, R. T. Cox, J. Cibert, H. Mariette, V. P. Kochereshko, M. Wiater, G. Karczewski, and T. Wojtowicz, Motion-dependent magnetic properties of excitons in CdTe, Phys. Rev. B **78**, 085204 (2008).

[22] J. J. Davies, L. C. Smith, D. Wolverson, A. Gust, C. Kruse, D. Hommel, and V. P. Kochereshko, Motion-enhanced magnetic moments of excitons in ZnSe, Phys. Rev. B **81**, 085208 (2010).

[23] L. C. Smith, J. J. Davies, D. Wolverson, H. Boukari, H. Mariette, V. P. Kochereshko, and R. T. Phillips, Wave-vector dependence of magnetic properties of excitons in ZnTe, Phys. Rev. B **83**, 155206 (2011).

[24] D. K. Loginov, V. P. Kochereshko, R. T. Cox, L. Besombes, H. Mariette, J. J. Davies, D. Wolverson, and L. C. Smith, Excitonic polaritons in transverse magnetic fields, Phys. Status Solidi B **247**, 1528 (2010)

[25] D. K. Loginov, Magnetic-field-induced polariton effects in light reflection spectra of structures with wide exciton quantum wells, Phys. Solid State **52**, 70 (2010).

[26] M. Altarelli and N. O. Lipari, Perturbation-theory investigation of the exciton ground state of cubic semiconductors in a magnetic field, Phys. Rev. B **7**, 3798 (1973).

[27] R. B. Dingle, Some magnetic properties of metals. II. The influence of collisions on the magnetic behavior of large systems, Proc. R. Soc. London Ser. A **211**, 517 (1952).

[28] E. L. Ivchenko, *Optical Spectroscopy of Semiconductor Nanostructures* (Alpha Science, Harrow, 2005).

[29] B. S. Monozon and P. Schmelcher, Optical absorption by excitons in semiconductor quantum wells in tilted magnetic and electric fields, Phys. Rev. B **82**, 205313 (2010).

[30] G. L. Bir and G. E. Pikus, *Symmetry and Strain Induced Effects in Semiconductors* (Wiley, New York, 1972).

[31] L. C. Lew Yan Voon and M. Willatzen, *The $k \cdot p$ Method: Electronic Properties of Semiconductors* (Springer, Berlin, 2009).

[32] In the structure under study, there is a small density of excess carriers, which broaden the exciton resonances in reflectance spectra. To compensate the carriers, we used a weak monochromatic illumination of the sample by radiation of a He-Ne laser.

[33] D. K. Loginov, E. V. Ubyivovk, Yu. P. Efimov, V. V. Petrov, S. A. Eliseev, Yu. K. Dolgikh, I. V. Ignatiev, V. P. Kochereshko, and A. V. Sel'kin, Interference of polariton waves in structures with wide GaAs/AlGaAs quantum wells, Fiz. Tverd. Tela **48**, 1979 (2006) [Phys. Solid State **48**, 2100 (2006)].

[34] A. V. Kavokin, J. J. Baumberg, G. Malpuech, and F. P. Laussy, *Microcavities* (Oxford University Press, New York, 2007).

[35] S. A. Markov, R. P. Seisyan, and V. A. Kosobukin, Spectroscopy of Excitonic Polaritons in Strained II–VI Semiconductor Structures with Wide Quantum Wells, Fiz. Tekh. Poluprovodn. **38**, 230 (2004) [Semiconductors **38**, 225 (2004)].

[36] D. K. Loginov, A. V. Trifonov, and I. V. Ignatiev, Effect of uniaxial stress on the interference of polaritonic waves in wide quantum wells, Phys. Rev. B **90**, 075306 (2014).

[37] V. A. Kiselev, I. V. Makarenko, B. S. Razbirin, and I. N. Ural'tsev, Size quantizing of excitons, Fiz. Tverd. Tela **19**, 1348 (1977) [Sov. Phys.—Solid State **19**, 1374 (1977)].

[38] A. V. Trifonov, S. N. Korotan, A. S. Kurdyubov, I. Ya. Gerlovin, I. V. Ignatiev, Yu. P. Efimov, S. A. Eliseev, V. V. Petrov, Yu. K. Dolgikh, V. V. Ovsyankin, and A. V. Kavokin, Nontrivial relaxation dynamics of excitons in high-quality InGaAs/GaAs quantum wells, Phys. Rev. B **91**, 115307 (2015).

[39] P. S. Grigoryev, A. S. Kurdyubov, M. S. Kuznetsova, I. V. Ignatiev, Yu. P. Efimov, S. A. Eliseev, V. V. Petrov, V. A. Lovtcius, and P. Yu. Shapochkin, Excitons in asymmetric quantum wells, Superlattices Microstruct. **97**, 452 (2016).

[40] M. M. Voronov, E. L. Ivchenko, V. A. Kosobukin, and A. N. Poddubnyi, Specific features in reflectance and absorbance spectra of one-dimensional resonant photonic crystals, Fiz. Tverd. Tela **49**, 1709 (2007) [Phys. Solid State **49**, 1792 (2007)].

[41] There are also several minor effects which complicate reflectance spectra. In particular, due to some difference in the dielectric constants there is an additional reflection at the heterostructure interfaces. Besides, there is smooth increase of the background dielectric constant in the spectral range around the anticrossing point related to strong exciton transitions in this range. We found that these small effects give rise to a smooth small change of the background reflection, which can be modeled by function: $\delta R_b = R_b\{1 - \exp[-(E - E_0)/\delta E]\}$ with $R_b = 0.048$, $E_0 = 1.516$ eV, and $\delta E = 0.0022$ eV.

[42] D. Schiumarini, N. Tomassini, L. Pilozzi, and A. D'Andrea, Polariton propagation in weak-confinement quantum wells, Phys. Rev. B **82**, 075303 (2010).

[43] J. J. Hopfield and D. G. Thomas, Theoretical and experimental effects of spatial dispersion on the optical properties of crystals, Phys. Rev. **132**, 563 (1963).

[44] S. Schumacher, G. Czycholl, F. Jahnke, I. Kudyk, H. I. Ruckmann, J. Gutowski, A. Gust, G. Alexe, and D. Hommel, Polariton propagation in shallow-confinement heterostructures: Microscopic theory and experiment showing the breakdown of the dead-layer concept, Phys. Rev. B **70**, 235340 (2004).

[45] E. V. Ubyivovk, D. K. Loginov, I. Ya. Gerlovin, Yu. K. Dolgikh, Yu. P. Efimov, S. A. Eliseev, V. V. Petrov, O. F. Vyvenko, A. A. Sitnikova, and D. A. Kirilenko, Experimental determination of dead layer thickness for excitons in a wide GaAs/AlGaAs quantum well, Fiz. Tverd. Tela **51**, 1818 (2009) [Phys. Solid State **51**, 1929 (2009)].

[46] E. S. Khramtsov, P. A. Belov, P. S. Grigoryev, I. V. Ignatiev, S. Yu. Verbin, Yu. P. Efimov, S. A. Eliseev, V. A. Lovtcius, V. V. Petrov, and S. L. Yakovlev, Radiative decay rate of excitons in square quantum wells: Microscopic modeling and experiment, J. Appl. Phys. **119**, 184301 (2016).

[47] R. G. Wheeler and J. O. Dimmock, Exciton structure and Zeeman effects in cadmium selenide, Phys. Rev. **125**, 1805 (1962).

[48] A. G. Zhilich and B. S. Monozon, Diamagnetic exciton in semiconductors with non-spherical bands, Fiz. Tverd. Tela **17**, 1343 (1975) [Sov. Phys. Solid State **17**, 866 (1975)].

[49] *Landolt-Bornstein Numerical Data and Functional Relationships in Science and Technology*, edited by O. Madelung, M. Schultz, and H. Weiss, New series, Vol. 17 (Springer-Verlag, Berlin, 1982); reprinted in O. Madelung (ed.), *Semiconductors-Basic Data*, 2nd ed. (Springer, New York, 1996).

[50] G. E. Stillman, D. M. Larsen, C. M. Wolfe, and R. C. Brandt, Precision verification of effective mass theory for shallow donors in GaAs, Solid State Commun. **9**, 2245 (1971).

[51] Following nonadiabatic terms should be included in the Hamiltonian of the diamagnetic exciton in the case of intermediate magnetic fields [3]: $\hat{H}_{na} = -\frac{\partial R_N^m}{\partial x}\frac{\partial W_{\alpha,\nu}}{\partial x} - W_{\alpha,\nu}\frac{\partial^2 R_N^m}{\partial x^2}$. The Schrödinger equation with these terms has no analytical solution so far.

[52] A. V. Kavokin, A. I. Nesvizhskii, and R. P. Seisyan, Exciton in a semiconductor quantum well subjected to a strong magnetic field, Fiz. Tekh. Poluprovodn. **27**, 977 (1993) [Semiconductors **27**, 530 (1993)].

[53] R. T. Collins, K. V. Klitzing, and K. Ploog, Photocurrent spectroscopy of GaAs/Al_xGa_{1-x}As quantum wells in an electric field, Phys. Rev. B **33**, 4378 (1986).

[54] P. W. Yu, G. D. Sanders, K. R. Evans, D. C. Reynolds, K. K. Bajaj, C. E. Stutz, and R. L. Jones, Electric field dependence of exciton transition energies in GaAs−Al_xGa_{1-x}As quantum wells studied by photocurrent spectroscopy, Phys. Rev. B **38**, 7796 (1988).